Sulfidation of synthetic biotites

JONATHAN L. TSO[1], M. CHARLES GILBERT AND JAMES R. CRAIG

Department of Geological Sciences
Virginia Polytechnic Institute and State University
Blacksburg, Virginia 24061

Abstract

Hydrothermal experiments have been conducted at 2000 bars in order to determine the composition of coexisting biotite and pyrrhotite. The sulfide–silicate compositional pairs were bracketed by using three layers within a single capsule: (1) pyrite + Fe-rich biotite in the top, (2) sanidine + magnetite in the middle, and (3) troilite + Mg-rich biotite in the bottom. At the conclusion of an experiment, the biotite in the top was found to have become more Mg-rich and the biotite in the bottom more Fe-rich, while a pyrrhotite of apparently homogeneous composition was found throughout the capsule.

Five equilibrium determinations at 700°C have been located:

$$(N)_{Po} = 0.928, \quad [Fe/(Fe + Mg)]_{Bi} = 0.496$$

$$0.936 \qquad 0.530$$

$$0.945 \qquad 0.541$$

$$0.947 \qquad 0.581$$

$$0.950 \qquad 0.585$$

and demonstrate that biotites become more Mg-enriched with increasingly sulfur-rich compositions of coexisting pyrrhotite.

The results can be applied to natural systems in which a pyrrhotite–biotite–magnetite–K-feldspar assemblage is present. Since sulfides are much more susceptible than Fe–Mg silicates to re-equilibration with decreasing temperature, silicate compositions can potentially be used as a measure of fS_2 and fO_2 during ore formation and metamorphism. This knowledge permits further calculation of chemical species in the vapor present during petrogenesis.

Introduction

The alteration of host-rock silicates by sulfur-bearing fluids during metamorphism of sulfide ore bodies has been recognized as yielding important clues in unraveling the history of these bodies. The petrogenesis of ore masses, however, is often obscured by the fact that sulfide mineral assemblages commonly do not reflect their peak conditions of metamorphism, due to relatively rapid re-equilibration at lower temperatures, as exemplified by the use of the pyrite–pyrrhotite geothermometer (Yund and Hall, 1969). As a result, determinations of the nature of sulfur-rich vapors based on compositions of pyrrhotite are

frequently not in agreement with evidence based on silicate mineral assemblages (Guidotti, 1970). Hence, much attention has been focused on silicates and oxides in the gangue and wall-rocks, which presumably do not re-equilibrate as rapidly as sulfides and still indicate, to a greater extent, the conditions of metamorphism.

One geochemical pattern previously recognized is the systematic decrease in $Fe/(Fe + Mg)$ in iron-magnesium silicates in the wall-rock with decreasing distances towards an ore-body. Such an effect for biotites has been documented by Staten (1976), Fullagar *et al.* (1967), and Harvey (1975). Meaningful interpretation of this pattern as an indication of silicate interaction with a sulfur-rich fluid in the ore zone requires that (1) equilibrium has been approached or
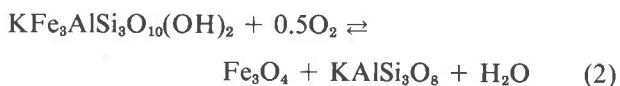
reached, and (2) iron was not preferentially added to or taken from the system or that the degrees of exchange can be calculated. A study by Bachinski (1976), however, did not show such a pattern for chlorites associated with metamorphosed sulfide deposits in Notre Dame Bay, Newfoundland. In this case, iron may have been introduced into the ore zone with the mineralizing fluids. This demonstrates that the preceding criteria must be considered very carefully. Nevertheless, in all these cases, Fe–Mg silicates are apparently responsive to the fugacity of sulfur during metamorphism or alteration.

Experimental studies of sulfide–silicate reactions have been done to only a limited extent. Kullerud and Yoder (1963, 1964) mixed various ferromagnesian silicates with sulfur and found, when starting with intermediate compositions, more magnesium-rich silicates plus sulfides in addition to various breakdown products at the conclusion of their runs. Whereas these earlier experiments were of a qualitative nature, Naldrett and Brown (1967) produced the first reversed experiments on sulfide–silicate reactions, equilibrating pyrrhotite and enstatite–ferrosilite solid solutions in evacuated silica glass tubes. This method was extended by Clark and Naldrett (1972) in a study of Fe–Ni partitioning between olivine and sulfide and by Rajamani (1976) for Co–Ni partitioning in orthopyroxene and sulfide. Hammarbäck and Lindqvist (1972) made hydrothermal experiments on biotites by using an oxide mix plus sulfur in gold tubes. While their results show a general trend of more sulfur-rich pyrrhotites coexisting with more magnesium-rich biotites, they did not demonstrate equilibrium. Popp *et al.* (1977), in experiments with coexisting pyrrhotite–orthoamphibole solid solutions, modified previous techniques so that reversibility in hydrothermal runs could be demonstrated. This method was used here in an attempt to equilibrate pyrrhotite and biotites along the join phlogopite–annite.

Ideally, the following reaction takes place for biotites:

$$KFe_3AlSi_3O_{10}(OH)_2 + 1.5S_2 \rightleftharpoons$$
$$KAlSi_3O_8 + 3FeS + H_2O + 1.5O_2 \qquad (1)$$
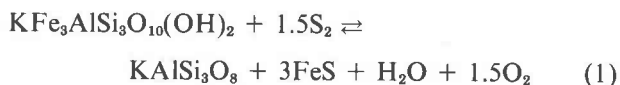
If magnetite is also present, then the reaction

$$KFe_3AlSi_3O_{10}(OH)_2 + 0.5O_2 \rightleftharpoons$$
$$Fe_3O_4 + KAlSi_3O_8 + H_2O \qquad (2)$$

must also occur. Combining reactions (1) and (2) yields the important equilibrium relation between magnetite and pyrrhotite,

$$Fe_3O_4 + 1.5S_2 \rightleftharpoons 3FeS + 2O_2 \qquad (3)$$

In reactions (1) and (2), the iron component in biotite breaks down upon reaction with the vapor to form a biotite enriched in magnesium. Concurrently, reaction (3) is a "sliding scale" buffer where the nonstoichiometric composition of pyrrhotite defines fS_2 and fO_2 if pure magnetite is present. The relationship between pyrrhotite composition and fS_2 has been experimentally determined by Toulmin and Barton (1964).

Under conditions of high fS_2, a fourth reaction will take place:

$$FeS_2 \rightleftharpoons FeS + 0.5S_2 \qquad (4)$$

Although pyrite was used as a starting material in all of the experiments, pyrrhotite was the only sulfide observed at the conclusion of most of the runs, indicating that the final run conditions yielded a fS_2 below this reaction.

Experimental methods

The experiments employed a triple-layer arrangement in a double gold capsule, as depicted in Figure 1. The inner capsule (1.02 mm outside radius) contained pure synthetic starting material + 4–5 mg distilled H_2O and was divided into the following layers: (1) Fe-rich biotite + pyrite, (2) magnetite + sanidine, (3) Mg-rich biotite + stoichiometric FeS (troilite) ± magnetite ± sanidine. By convention, this study will label layer 1 as the top, layer 2 as the middle, and layer 3 as the bottom. The constituents of the individual layers were mixed for several minutes by hand in an agate mortar and carefully packed into the tube. The tube was welded shut, and the vacant portion at the top of the capsule was flattened and bent as an indicator of the orientation of the layers.

This capsule was placed in a larger gold capsule
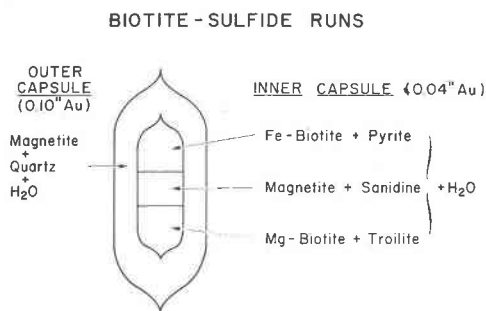
BIOTITE – SULFIDE RUNS

Fig. 1. Capsule arrangement showing the three layers, their constituents, and the outer capsule.

(2.54 mm outside radius) and surrounded by magnetite + quartz + 30 mg distilled H_2O. The purpose of the outer capsule and its "buffer" is twofold: (1) to help isolate physically the inner capsule from the environment of the pressure vessel; (2) to help provide limitations on the fO_2 of the charge, with the upper limit being the magnetite–hematite buffer curve and the lower limit being the fayalite–magnetite–quartz buffer curve. No hematite or fayalite was ever found in the outer capsule after a run.

The capsules were run in standard cold-seal hydrothermal apparatus, in which temperatures were measured by bare-wire chromel–alumel thermocouples calibrated at one atm against the melting point of NaCl (800.5°C) and CsCl (646°C). The accuracy of measurement is estimated at ±5°C. Pressures were measured by factory-calibrated Heise Bourdon-tube gauges which are assumed accurate to ±50 bars.

Runs were quenched by blowing a stream of air over the vessels for one minute and then immersing them in cold water. On opening the inner capsule, a stronger odor of H_2S, when compared to the outer, signified the effective sealing of the capsule. An examination of the charge showed that the three layers were easily distinguished by their color. The layers were then separated and saved for analysis.

A bracket resulted when a run yielded: (1) a single homogeneous composition of pyrrhotite throughout the capsule; (2) Mg-enrichment of the Fe-rich biotite (top layer); and (3) Fe-enrichment of the Mg-rich biotite (bottom layer).

Equilibrium compositions of the coexisting biotite–sulfide assemblage were determined by using the measured pyrrhotite composition and the mid-points between the most Mg-rich biotite observed in the top and the most Fe-rich biotite in the bottom.

Strictly speaking, separation of the starting materials into layers was not necessary, as a single biotite and a single pyrrhotite should always be produced at equilibrium. However, biotite is usually sluggish in these reactions, and approached but rarely reached the determined equilibrium composition. Accordingly, separation of biotite into layers facilitated observation of compositional changes.

Finally, magnetite and sanidine were present at the conclusion of all bracketing runs even where these two constituents were not mixed into the starting layers.

Synthesis of starting material

Biotite

The biotites used in this study lie compositionally along the join annite–phlogopite. Fe/(Fe + Mg) as

used below represents mole percent "ideal annite," assuming all iron to be octahedral. Variation in Fe^{3+}/Fe^{2+} is accounted for in determination of physical properties and discussed in the section on analysis of run products. Both end members plus two intermediate compositions [$KMg_2FeAlSi_3O_{10}(OH)_2$ and $KMgFe_2AlSi_3O_{10}(OH)_2$] were synthesized from oxide-glass mixes prepared as follows: A glass of the composition $K_2Si_4O_9$ was made from K_2CO_3 prepared from $KHCO_3$ (Fisher lot 712479) and SiO_2 (Corning lump cullet #7940) treated with nitric acid. The glass was prepared as described in Schairer and Bowen (1955), and was found to be optically homogeneous after several crushing and melting cycles. It has an index of refraction of 1.495±.001. γ-alumina was produced by heating $AlCl_3 \cdot 6H_2O$ (Fisher lot 711038) in a silica-glass boat at 700°C until a constant weight was achieved. The material was then held at 900°C for 2 hours. No aluminosilicates were observed in X-ray powder diffractograms or optical searches. MgO (Materials Research Corporation job no. 30635) was dried at 1000°C for 1–2 hours. Fe-sponge (Johnson Mathey and Company) was checked for oxygen content by weighing a few grams in a silica-glass boat, reducing it in an H_2 flow at 500°C for 30 hours, and reweighing it. An oxygen-content correction factor was then calculated and applied to the Fe-sponge used in the mix. These materials were combined with more SiO_2 glass to give the proper compositions of biotite and were mixed in a mechanical agate mortar under alcohol for about 4 hours until judged homogeneous.

The iron-bearing mixes plus distilled H_2O were loaded into $Ag_{70}Pd_{30}$ tubes and run at various temperatures and 1000 bars methane with graphite filler-rods. It was found necessary to regrind and reload the charges once to produce runs of ≥95 percent biotite. Phlogopite was synthesized in gold tubes (2.54 mm outside radius) in standard hydrothermal apparatus at 700°–800°C, 2000 bars for 7 days. The charge consisted of >98 percent biotite.

Portions of the Fe-bearing biotites were annealed in Pt tubes at the Ni–NiO buffer for one week for comparison with the physical-property data of Wones (1963), using his regression curves for the relations between the physical properties and Fe/(Fe + Mg) of biotite. The data obtained (Table 1) show good agreement between the observed $d(060/\overline{3}31)$ and the d value calculated from his curves. The best fit between measured and calculated values was obtained if the quadratic rather than the linear expression of Wones was used. The comparison between the measured γ and calculated γ also shows

Table 1. Comparison of measured physical properties of annealed biotites (NNO, 600°C, 2000 bars) and predicted physical properties and compositions from Wones (1963); and unit cell dimensions

Composition of starting mix Fe/(Fe + Mg)	Measured d(060/$\overline{3}$31)	Predicted d(060/$\overline{3}$31)	Predicted Fe/(Fe + Mg) from measured d(060/$\overline{3}$31)	Measured n_γ	Predicted n_γ	Predicted Fe/(Fe + Mg) from measured n_γ	Unit Cell Parameters				
							a(Å)	b(Å)	c(Å)	β	V(Å³)
*0.0	1.5351(5)	1.5348(4)	0.012	#1.583	1.581(3)	0.022	5.319(2)	9.193(3)	10.313(3)	99.90(3)	496.7(2)
	[a]1.5349(6)	--	0.004	#1.581	--	0.002	5.326(6)	9.210(9)	10.311(9)	100.17(13)	497.77
	[b]∞1.5346(2)	--	-0.008	†1.583(1)	--	0.022	5.317(1)	9.203(2)	10.310(2)	99.92(1)	496.9(1)
							[b]5.318(2)	9.206(5)	10.308(2)	99.83(2)	497.2(3)
0.33	1.5429(5)	1.5427(4)	0.338	#1.617	1.616(3)	0.339	5.349(2)	9.245(4)	10.311(3)	99.95(3)	502.2(2)
0.67	1.5503(5)	1.5498(4)	0.696	#1.657	1.657(3)	0.674	5.371(2)	9.297(3)	10.304(3)	99.95(3)	506.7(2)
1.00	1.5572(5)	1.5556(4)	1.103	#1.696	1.700(3)	0.971	5.395(2)	9.340(3)	10.300(3)	100.00(2)	511.1(2)
	[c]1.5568	--	1.077	--	--	--	5.381(10)	9.330(6)	10.285(20)	99.93(25)	--
	[d]1.5550(10)	--	0.963	#1.697	--	0.978	--	--	--	--	--

[a] Wones (1963)

[b] Hewitt and Wones (1975)

[c] Rutherford (1973)

[d] Eugster and Wones (1962)

*not annealled at 600°C, NNO

∞ calculated d($\overline{3}$31) from regression equation of Wones (1963)

† calculated n_γ from regression equation of Hewitt and Wones (1975)

± 0.002

agreement well within the error of measurement. Measurements were aided by use of a wavelength interference filter employing a single-variation technique (Bloss, in preparation). Measurements of a number of grains show an essentially homogeneous composition of samples.

Table 1 also lists unit-cell dimensions assuming a 1M polytype, although the measured powder reflections agreed well with either a 1M or 3T polytype. The 1M polytype was used in order to be consistent with values reported by Eugster and Wones (1962), Wones (1963), and Hewitt and Wones (1975). Several low-intensity biotite peaks, however, did not agree with the 1M or 3T structure. From the discussion of Hewitt and Wones (1975), these peaks are thought to indicate the presence of a small portion of $2M_1$ mica. The presumed small free-energy difference between these polytypes is not expected to significantly affect the results of the experiments.

K-feldspar

K-feldspar was produced by mixing together $K_2Si_4O_9$ glass, SiO_2 glass, and γ-alumina, loading into gold capsules + H_2O and running at 750°C, 1000 bars, for 3 days. Results were 99 percent feldspar. Unit-cell dimensions obtained from X-ray powder methods are: $a = 8.602(1)$, $b = 11.302(2)$, $c = 7.179(1)$Å and $\beta = 116.02(1)°$. The powder pattern agrees with that given by Borg and Smith (1969) for high sanidine.

Quartz

Quartz used was Fisher (lot 711367) silica (140 mesh), which was treated in HCl and then H_2SO_4.

Pyrite and troilite

Starting sulfides were synthesized from ASARCO sulfur chips (99.999 percent pure) and iron sponge (Johnson Mathey and Company, reduced at 900°C with an H_2 flow) in evacuated silica-glass tubes.

Magnetite

Magnetite used was ferric–ferrous oxide black (Fisher lot 783353). An X-ray and reflected-light study showed only magnetite present. This material was not annealed.

Wüstite

Wüstite was prepared by heating appropriate mixtures of Fe-sponge and dried ferric oxide (Fisher lot 763159) in an evacuated silica-glass tube at 850° for 3 days. No Fe-silicates were observed by optical methods.

Analysis of run products

Run products were identified and characterized by transmitted and reflected-light studies, and X-ray diffraction, with a Norelco or Picker powder diffractometer. For peak-position determinations, a CaF_2 internal standard [$a = 5.5632(14)$Å] was used.

Biotites

Two methods of determination of composition were used. Firstly, we measured d values of the composite $\overline{3}31$–060 peak, in conjunction with the regression equations of Wones (1963). As the Wones equations are applicable only to biotites at the oxygen fugacity defined at various solid buffers, and with the oxygen fugacity of the sulfidation runs intermediate between that defined by the solid buffers, a method of interpolation was necessary. A plot of oxygen fugacity against the apparent composition [Fe/(Fe+Mg)] at 600°C for a single $d(060/\overline{3}31)$, calculated at various solid buffers using the equations of Wones (1963) and the oxygen fugacity data listed in Huebner (1971), reveals that, even at the most Fe-rich compositions, the line of constant $d(060/\overline{3}31)$ is approximately a straight line between FMQ and MH (the actual plot appears in Tso, 1977). Since all the sulfidation experiments fall between NNO and MH, a linear interpolation between NNO and MH was considered valid. Secondly, the γ of biotite was measured, again using the regression curves of Wones (1963) and interpolating between curves when necessary.

In oils, the biotites were seen to be platelets ranging from less than 1 μm to 10 μm in length, showing pleochroism and a suggestion of zoning in the coars-

OPTICAL AND X-RAY MEASUREMENTS
OF BIOTITE COMPOSITION FOR A SINGLE RUN

RUN #30, 700°C, 2000 b, $N_{po} = 0.947$
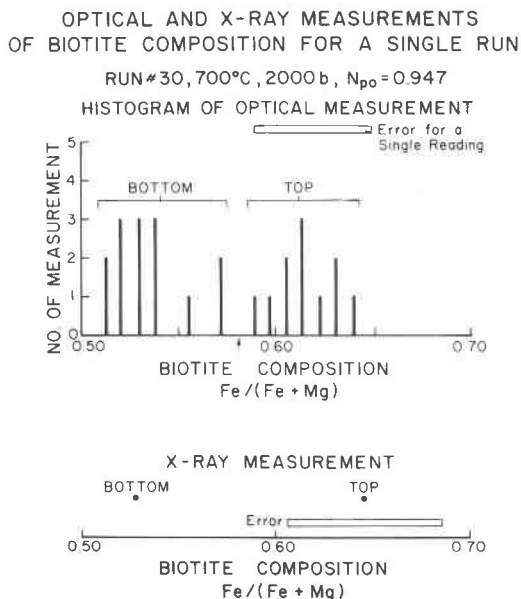HISTOGRAM OF OPTICAL MEASUREMENT

X-RAY MEASUREMENT

Fig. 2. Comparison of optical and X-ray measurements for run #30, 700°C, 2000 bars. The arrow on the optical measurement diagram is the location of the inferred biotite composition: the midpoint between the most magnesium-rich biotite observed from the top and the most iron-rich biotite from the bottom.

est grains from the top layer. Figure 2 shows the result of the measurement of a number of grains (4–8 μm) from a single typical reversal experiment. A scatter of compositions was observed. However, the midpoint of the reversal bracket is considered to lie between the most Mg-rich biotite in the top layer and the most Fe-rich biotite in the other layer. The reversal bracket is consistent with that determined by X-ray powder method but carries a smaller uncertainty.

Finally, the assumption was made that the biotites do not differ in composition, at termination of bracketing runs, from those along the phlogopite–annite join. For natural biotites, Banks (1973) has observed up to 345 ppm of sulfur in some form. Such concentrations, if present in our biotites, are assumed not to affect significantly the physical or chemical properties. No discrepancies between optical and X-ray determinations from Wones (1963) that would indicate an aluminous biotite (Hewitt and Wones, 1975) were observed for the equilibrium runs.

Pyrrhotite

In reflected light, pyrrhotite was seen as equant, untwinned grains up to 50 μm across, commonly containing blebs of magnetite or rarely pyrite. Compositions were determined by means of the $d(102)$ peak, using the relation between d value and composition given by Yund and Hall (1969). The compositions of pyrrhotite are expressed as N, the mole fraction of FeS in the system FeS–FeS_2 (Toulmin and Barton, 1964). Only runs in which the compositions were within an N value of ±0.003, the experimental uncertainty of Yund and Hall, were used. Occasionally, for those compositions close to troilite, the peak coincided with one for magnetite or was too weak to measure accurately. In these cases, the runs were not used for equilibrium determinations.

A number of runs contained pyrite in the top and bottom. Pyrrhotite compositions in these runs frequently showed significant differences between the layers. These pyrrhotites were assumed not to reflect their equilibrium compositions but to have exsolved some, if not all, of the pyrite on quenching. As a result, these runs were not used in defining brackets.

Pyrite

Pyrite was found only in the most sulfur-rich runs and normally was accompanied by Al-rich magnetite and langbeinite [$K_2Mg_2(SO_4)_3$]. In reflected light, it appears as discrete grains up to 30 μm or as smaller blebs in or adjacent to magnetite or pyrrhotite. Pyrite

is more commonly found in the layer to which it was added, but its presence in the other layer signifies that not all can be considered as unreacted starting material.

Magnetite

In polished section magnetite appeared similar to the starting material, being extremely fine-grained (*i.e.* less than several microns); thus it was difficult to determine optically but could be clearly identified by X-ray methods.

In several experiments at high fS_2 at 800°C the magnetite is coarser (up to 30 μm), occurring as blebs or euhedral grains in pyrrhotite or pyrite and also as discrete grains. Under close observation, these magnetites sometimes exhibited weak reddish internal reflections. Because as much as 15 weight percent magnesioferrite component occurs in magnetite of pyrite–pyrrhotite ores in Sweden (Annersten, 1969), partial microprobe analyses (Table 2) of the synthetic magnetite were carried out for Fe, Mg, and Al to check for possible solid solution. The analyses showed minor amounts of Mg but significant enrichment in Al. The significance of the high Al content of magnetites in the presence of pyrite is not known, but the occurrence of pyrite in these runs and the absence of demonstrated pyrrhotite equilibration precluded use of these experiments as "brackets." The runs are not included in the equilibrium data table.

K-feldspar

K-feldspar is either irregularly shaped or blocky (especially in the middle layer), the average size being 5–10 μm. Qualitative microprobe data of a few random samples show negligible iron content. Kalsilite and leucite were not detected.

Other products

Runs with high fS_2 contained phases in addition to pyrite. None of these runs was used to determine equilibrium, due to the presence of pyrite. These products were especially prevalent in a few reconaissance experiments at 800°C. Some of these 800°C runs also showed pyrite as an apparent quench product. Complete description and data are given in Tso (1977).

Langbeinite, $K_2Mg_2(SO_4)_3$, was found at both 700° and 800°, usually in association with aluminous magnetite and pyrite. Because it was extremely fine-grained, it was difficult to identify optically but was seen clearly in the X-ray powder pattern.

Quartz and pyroxene were observed in only one run and occurred with langbeinite and Al-magnetite. In this run, biotite broke down completely and no sanidine was detected. Quartz averaged about 10 μm in size, although one grain was estimated to be 50 μm. Pyroxene was less than 2 μm and could be positively identified only by X-ray techniques.

Determination of the oxygen fugacity

Oxygen fugacity was not externally buffered or directly measured but was calculated from equation (3):

$$Fe_3O_4 + 1.5S_2 \rightleftarrows 3FeS + 2O_2 \qquad (3)$$

Experimental determination of the reaction was

Table 2. Microprobe analyses of magnetites (weight percent)

Run no.	29,mid	36,mid	36,top	*22,mid	*22,mid	*37,mid	*37,mid
T°C	700	800	800	800	800	800	800
Al_2O_3	0.00	0.12	0.35	7.23	5.00	2.07	1.91
FeO	87.66	88.63	88.32	82.77	82.96	85.00	86.20
MgO	0.27	0.55	0.55	0.70	0.64	0.87	0.73
Total	87.94	89.30	89.23	90.71	88.61	87.94	88.84

all Fe was calculated as Fe^{2+}

*pyrite was a run product.

Table 3. Fayalite–magnetite–quartz–pyrrhotite equilibria; 2000 bars

T°C	Pyrrhotite Composition (N±0.002)			$\log f_{S_2}$ (±0.35)	$\log f_{O_2}$ (±0.20)
	Upper	Lower	Average		
600	.9608	.9604	.9606	-5.39	-19.76
650*	.9621	.9601	.9611	-4.71	-18.20
675*	.9617	.9617	.9617	-4.41	-17.49
700*	.9650	.9642	.9646	-4.37	-16.81
725*	.9661	.9636	.9649	-4.08	-16.16
750	.9629	.9625	.9627	-3.56	-15.55
800	.9629	.9638	.9634	-3.06	-14.41

*Determined by Popp et al. (1977).

made by Popp *et al.* (1977). Their data plus our new experiments have been used to locate the magnetite–pyrrhotite curve in log f_{O_2}–log f_{S_2} space.

Experiments at 600°, 750°, and 800°C were performed using the triple-layer method, with fayalite + quartz + magnetite + pyrite in one end of the capsule, fayalite + quartz + magnetite + troilite in the other end, and fayalite + quartz + magnetite in the middle layer and outer capsule. After runs of one week, fayalite + magnetite + quartz + pyrrhotite

was present throughout, with the composition of pyrrhotite appearing everywhere homogeneous. Presence of this assemblage defines a point on the magnetite–pyrrhotite curve where the composition of pyrrhotite defines f_{S_2}, and the assemblage fayalite–quartz–magnetite defines f_{O_2}.

Using the equation for the relationship between $d(102)$ and N of pyrrhotite given by Yund and Hall (1969) and the equation for N, log f_{S_2}, and log a_{Fes}^{Po} from Toulmin and Barton (1964), corrected to 2000 bars, the data in Table 3 were generated. Oxygen fugacity was determined by means of the equation of Hewitt (1978). The data of Popp *et al.* (1977) have been modified to be in accord with the above relations. Once the experimental point has been located, K may be calculated and the slope of the line can then be determined from the equation:

$$\log K = 2 \log fO_2 + \log a_{Fes}^{Po} - 1.5 \log fS_2 \quad (5)$$

for a given fS_2 in fO_2–fS_2 space. The curve location at 700°C, 2000 bars reported by Popp *et al.* (1977) is compared in Figure 3 with that calculated using thermodynamic data [see Popp *et al.* (1977) for the method of calculation] and with that based on our methods. Our location is closer to the calculated curve than that of Popp *et al.*, but well within the limits of error established for these curves. The slight curvature in the line is due to the changing activity of pyrrhotite. Figure 4 is a plot of all the curves for the various temperatures.
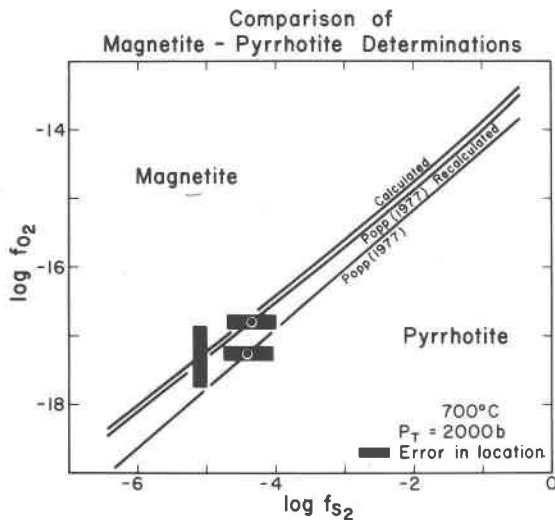

Fig. 3. Comparison of locations for the magnetite–pyrrhotite curve, 700°C, 2000 bars. Dots represent location of the determined equilibrium assemblage fayalite–quartz–magnetite–pyrrhotite. Calculated from thermodynamic data; Popp (1977)—position given by Popp *et al.* (1977); Popp (1977) recalculated—a redetermining of the data of Popp *et al.* (1977) using the equation for log $f O_2$ from Hewitt (1978) and the d value *vs.* composition equation given by Yund and Hall (1969).
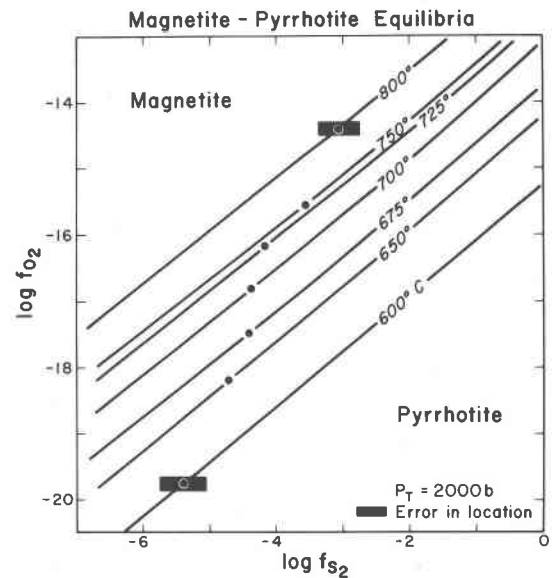

Fig. 4. Experimental determinations for the magnetite–pyrrhotite curve on a log $f O_2$–log $f S_2$ plot. Dots indicate the experimental data points.

Table 4. Compositional determinations of run products—pyrrhotite composition (N) (±.003) biotite composition [Fe/(Fe + Mg)] X-ray (±.04)

Run No.	Time	Final Upper	Final Lower	Starting Upper	Starting Lower	Final Upper	Final Lower
				600°			
a,b 10	354h	.9379	.9258	.67	.33	.146	.235
b 15	335h	.9210	.9160	.67	.33	.442	.398
c 21	501h	.9229	weak	.67	.33	.432	.365
c 23	547h	.9221	.9168	.33	0.0	.341	.114
31	359h	.9451	.9466	.67	.33	.517	.442
32	358h	.9280	.9286	.67	.33	.558	.490
				700°			
a,b,c 11	351h	.9200	.9206	.67	.33	.297	.257
b,c 16	343h	.9371	.9371	.67	.33	.492	.474
a 24	787h	.9186	weak	.33	0.0	.273	.180
26	378h	.9223	.9263	.33	0.0	.401	.376
28	362h	.9282	.9303	.67	.33	.491(.516)	.415 [.475]
d 29	387h	.9438	.9452	.67	.33	.537(.570)	.492 [.511]
d 30	417h	.9472	.9466	.67	.33	.645(.589)	.528 [.572]
33	359h	.9373	.9360	.67	.33	.534(.530)	.503 [.530]
d 34	357h	.9518	.9499	.67	.33	.629(.593)	.588 [.576]

a pyrite present after quenching
b no middle layer
c magnetite not detected
d wustite in middle layer
()=most Mg-rich and []=most Fe-rich biotite observed using optical methods

In actual practice, for a sulfidation run, the pyrrhotite compositions were determined from the $d(102)$ value with log fS_2 and log a_{Fe}^{Po}s calculated as previously described. Using the value of K determined for the appropriate temperature of the run, the value of log fO_2 for each run was then calculated from equation 5. The composition of biotite was then corrected to fO_2 by a linear interpolation of the measured physical properties between the regression curves given in Wones (1963).

Discussion of results

Table 4 lists the results of the pertinent experiments on the sulfidation of biotites. Runs may be categorized into several types: (1) compositions of biotites shifted in the same direction, either to more Fe-rich or more Mg-rich, (2) composition of one layer moved from Fe-rich to more Mg-rich while composition of the other layer moved from Mg-rich to more Fe-rich, or (3) no change was detected in one layer but change was detected in the other. The experiments considered to determine tie-lines meet the following criteria: (1) pyrrhotite compositions (N) between the top and bottom must be within ±0.003, (2) the final composition of biotite is intermediate between the starting compositions of the top and bottom, and (3) magnetite plus sanidine is present.

Preliminary compositions based on X-ray determinations were useful as a guide to the trends of the experiments, but proved to be misleading when a mixture of two biotites of different composition was used as starting material in either the top or bottom layer. X-ray analyses showed essentially average compositions, but optical examination revealed a wide range of Fe/(Fe + Mg) values to be present. Appreciable overlap of compositions from top to bottom was observed, probably due to sluggishness of biotite equilibration, and hence, no bracket could be assigned. The data of these experiments are available in Tso (1977).
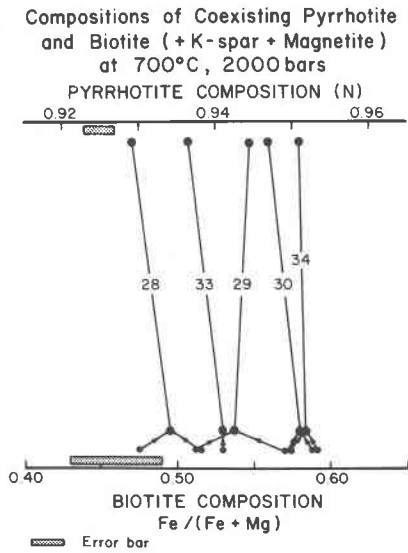
Fig. 5. Biotite–pyrrhotite equilibria at 700°C and 2000 bars. The biotite compositions are the averages of the optically observed most Mg-rich biotite in the top and the most Fe-rich composition of the bottom. Arrows indicate bracketing compositions of the top and bottom. Pyrrhotite compositions are average N values between top and bottom. Run numbers are listed on the tie-lines.

Several points of technique require additional discussion. In order to control roughly the fS_2, varying amounts of sulfide, and occasionally mixtures of pyrite + troilite, were used in the top layer. This method

was found to be fairly successful, but better control was achieved by mixing synthetic wüstite in the middle layer in place of magnetite. This resulted in a lower value of fS_2. In all such runs, magnetite + pyrrhotite was the final assemblage. Addition of hematite should allow higher fS_2 conditions, but in our experiments this was not found necessary.

Five well-reversed tie-lines at 700°C and 2000 bars are plotted in Figure 5. The trend of increasing magnesium enrichment in the silicate as a function of increasing sulfur content of pyrrhotite is similar to that found for orthoamphiboles by Popp et al. (1977). Figure 6 represents the system on a $\log fO_2$–$\log fS_2$ plot at 700°C and 2000 bars, using the experimentally-located magnetite–pyrrhotite curve and assuming stoichiometric magnetite and K-feldspar. The biotite compositional fields are shown as contours representing reactions (1) and (2), with the determined biotite composition labeled on each line. The intersection of the lines representing reactions (1) and (2) are the locations of the five experimental points in fO_2–fS_2 space. The curves for reaction (2), as will be shown below, can be extrapolated horizontally from the experimental points to the $\log fO_2$ axis, essentially the sulfur-free system. There, the variations of biotite composition as a function of fO_2 can be compared with the study of Wones and Eugster (1965), in which the composition of biotite (reaction 2) was deter-
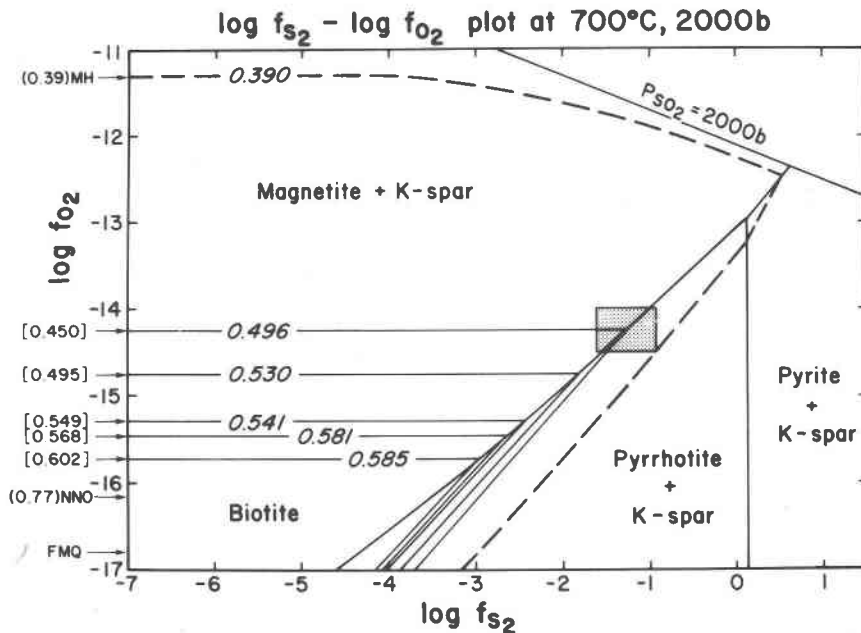

Fig. 6. Biotite stability on the $\log fO_2$–$\log fS_2$ plot at 700°C, 2000 bars. Positions of the buffers MH, NNO, and FMQ are indicated by arrows on the $\log fO_2$ axis. Numbers in parentheses are the compositions of biotite with magnetite + sanidine taken from Wones and Eugster (1965). Dashed line is the extrapolated curve of a biotite of Fe/(Fe + Mg) of 0.39. Numbers in brackets represent calculated Fe/(Fe + Mg) from the solution model of Wones and Eugster (1965).

mined as a function of temperature and pressures of 1036 and 2070 bars, using solid buffers. Their experimental compositions for 2070 bars are in parentheses next to the arrows signifying the position of the solid buffers.

Log fH_2 can be calculated for all of the equilibrium experiments. This allows a comparison of the experimentally-determined compositions of biotite with predicted compositions based on the solution model of Wones and Eugster (1965). The compositions obtained in this manner for their value of X_1 are in brackets on Figure 6 and are well within the experimental error of this study. A comparison of the revised interrelation of annite stability in Wones (1972) is less favorable. For instance, run #28, which has an equilibrium composition of 0.496 Fe/(Fe + Mg) calculates as only 0.288 using his equation. The conditions used in the sulfidation experiments, however, were more oxidizing than those directly considered by Wones. Furthermore, the largest difference between the experimental compositions of this study and those calculated from Wones occurs at higher fO_2. Our experiments are consistent with the experimental compositions of Fe/(Fe + Mg) of Wones and Eugster (1965), using the physical properties measured by Wones (1963). Apparently, current solution models do not adequately describe biotites with appreciable ferric component.

Composition of the vapor

For an H–O–S vapor, the value for fH_2 can be calculated by the method of Eugster and Skippen (1967), assuming ideal mixing, and given a specified fO_2 and fS_2. From this, one may calculate the fugacities of any of the vapor species, as has been done by Popp *et al.* (1977) and in this paper. Values for the equilibrium constants were taken from the JANAF Tables (1971), and values for fugacity coefficients of H_2 were obtained from Shaw and Wones (1974), of H_2O from Burnham *et al.* (1969), of H_2S from Ryzhenko and Volkov (1971), and of SO_2 estimated from the reduced variable charts of Hougen *et al.* (1964). All other species were assumed to have a fugacity coefficient equal to unity. The species for which calculations were made were H_2, H_2O, SO_2, SO, H_2S, HS, and H_2SO_4. Figure 7 is a series of maps calculated at 600°, 700°, and 800°C showing lines of constant fH_2. From any point on these maps, one can easily estimate the fugacity of any of the species anywhere on the diagram by use of the proper equilibrium constants.

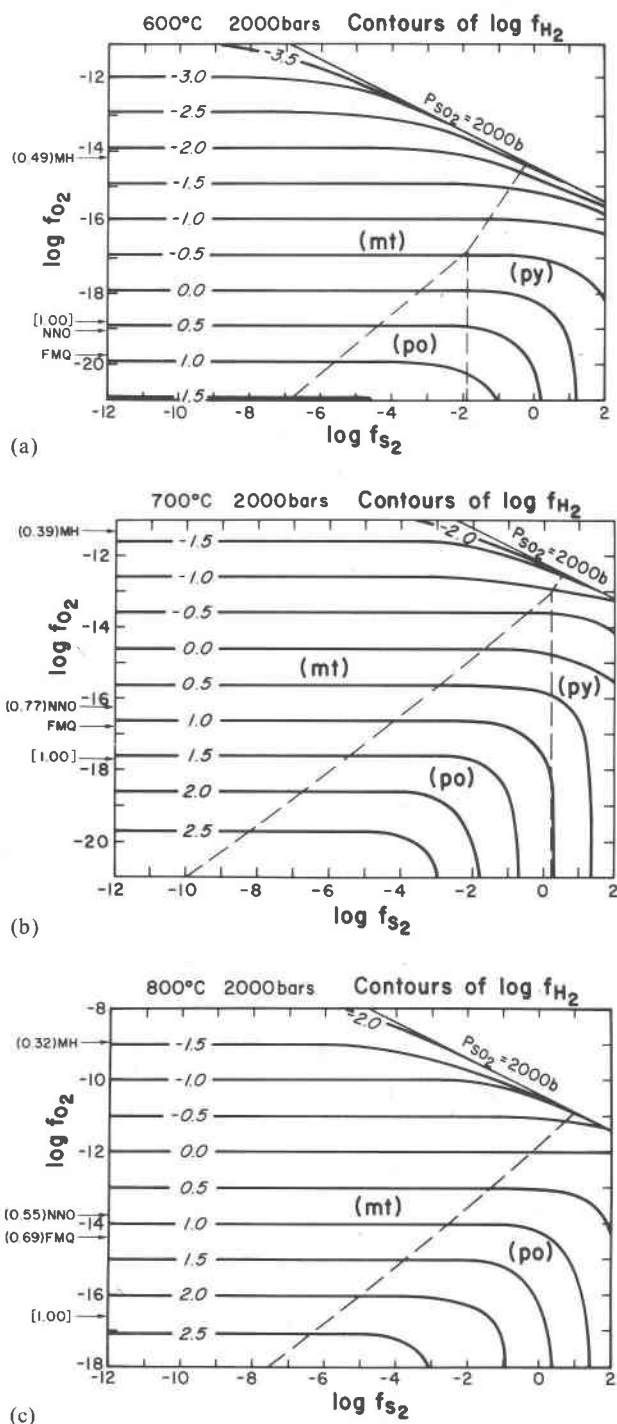Using Figure 7b as an example, several points are evident. There is a region at relatively high $\log fO_2$–

Fig. 7. (a) Lines of constant $\log fH_2$ on a $\log fO_2$–$\log fS_2$ plot for 600°C. Dashed lines represent oxide–sulfide equilibria. (b) Lines of constant $\log fH_2$ on a $\log fO_2$–$\log fS_2$ plot at 700°C. (c) Lines of constant $\log fH_2$ on a $\log fO_2$–$\log fS_2$ plot at 800°C. Abbreviations are as follows: mt = magnetite; po = pyrrhotite; py = pyrite. Numbers in parentheses represent location of the experimentally-determined compositions of intermediate biotite at various solid buffers (Wones and Eugster, 1965). The numbers in brackets represent the location of annite by Rutherford (1973).

log fS_2 where the calculated partial pressure of SO_2 exceeds the total pressure of 2000 bars. This area is not, therefore, physically realizable. Note also that at 700° the assemblage magnetite + hematite + pyrite is in this area.

Reaction (2) may be rewritten:

$$KFe_3AlSi_3O_{10}(OH)_2 \rightleftharpoons Fe_3O_4 + KAlSi_3O_8 + H_2 \quad (6)$$

As a result, for a given composition of biotite, pure magnetite, and K-feldspar:

$$\log K = \log fH_2 - \log a_{Fe}^{Biot} \quad (7)$$

Therefore, for a given biotite composition, the curve for reaction (6) should parallel the log fH_2 contours on the log fO_2–log fS_2 plot, which are essentially straight horizontal lines over most of the magnetite-dominated portion of the diagram. Extrapolation from the experimental points to the fO_2 side should therefore be possible. However, a magnesium-rich biotite of Fe/(Fe + Mg) of 0.39 stable at the magnetite–hematite buffer (Wones and Eugster, 1965) would not extrapolate linearly, but would be limited by the existence of the area of high SO_2. The biotite compositional curve (dashed line on Fig. 6) bends down toward lower fO_2 as this area is approached.

The fact that the results of these experiments show agreement with the experimental data of Wones and Eugster (1965) is an independent indication that approach to equilibrium has been achieved.

Incompatibility with the preceding criterion indicates a non-attainment of equilibrium. Hammarbäck and Lindqvist (1972) reported two runs as having pure phlogopite (with magnetite + sanidine + pyrrhotite and having log fS_2 of −5.2 and −4.7 and 575°, 1600 atm). These compositions should show an oxide–sulfide assemblage of magnetite (with possible hematite) and pyrite, rather than magnetite–pyrrhotite. In addition, the crossing of tie lines shown in their data is an indication of nonequilibrium. Note, however, that Hammarbäck and Lindqvist did not claim that their experiments represented equilibrium.

Geological applications

Biotites are important gangue minerals in sulfide ores. Unfortunately, chemical data are lacking on biotites in many assemblages to which our experimental data could be applied. However, whenever coexisting sulfides and biotites have been investigated, interaction during crystallization appears to have occurred. This is true whether the assemblages are in ore deposits, regional metamorphic terranes, or igneous rocks.

Putnam (1972, 1973) described biotites coexisting with K-feldspar and pyrrhotite ± magnetite in the Rocky Hill Stock, California. The temperature of crystallization was estimated at 700°C at 1.5–2.0 kbar, with the biotite compositions falling in the range 0.43–0.50 mole fraction of annite. This is consistent with his oxygen fugacity estimate of 10^{-14} to 10^{-16} atmospheres, as seen in Figure 6. His estimate of log $fS_2 = 10^{-2}$ atmospheres correlates well with the expected log fS_2 of −1.3 to −3.3 in Figure 6. From Figure 7b, this would correspond to a log fH_2 of −0.3 to +0.7 on the magnetite-pyrrhotite curve, and would permit the calculation of the fugacities of the remaining vapor species in an H–O–S system.

Beane (1974) compiled data on biotites from the alteration zones of porphyry copper environments, and has proposed a geothermometer based upon the oxy-component and phlogopitic mole fraction of the biotite. His data show a relationship between the amount of phlogopite component $[KMg_3AlSi_3O_{10}(OH)_2]$ and a hypothetical component, proton-deficient oxyannite $[KFe_3^{3+}AlSi_3O_{12}(H_{-1})]$, such that with increasing temperature at a constant X_{Phl}, the amount of X_{P-doxy} increases. Our study does not yield an independent estimate of ferrous and ferric iron in biotite and thus unfortunately limits direct correlation with Beane's study.

In metamorphic terranes Guidotti (1970) has made partial chemical analyses of biotites from the southeastern portion of the Oquossoc 15' Quadrangle, Maine. His study showed that, within the upper sillimanite zone, the addition of 6–7 modal percent sulfide correlates with a marked decrease of Fe/(Fe + Mg) of biotite. For instance, biotites in mica schists that contain no sulfide have an Fe/(Fe + Mg) atom percentage of 65.8 (location 101), whereas less than 200 m away biotites in mica schists with 6 modal percent sulfide have an Fe/(Fe + Mg) percentage of 28.2 (location 100).

Robinson and Tracy (1977) have also demonstrated correlation between types of sulfide–oxide–silicate assemblages and Fe content of biotite in pelitic rocks of central Massachusetts. These rocks are believed to have equilibrated at 650°–700°C at 6 kbar. For example, with ubiquitous graphite, quartz, sillimanite, K-feldspar, and plagioclase, the silicates in the assemblage pyrrhotite, garnet, biotite, ilmenite have a higher Fe/(Fe + Mg) than those of the assem-

blage pyrrhotite, pyrite, cordierite, biotite, rutile. The results clearly relate the Fe-depletion of silicates with more sulfur-rich conditions.

Staten (1976) has shown systematic changes in biotite composition from the Great Gossan Lead, SW Virginia as a function of distance from an ore toward pelitic–psammatic schists. Here the Fe/(Fe + Mg) percentage is 26.4 in the ore zone; 40.4, five feet into the country rock; and 47.7, seven feet or more into the country rock, which indicates a relatively narrow alteration around the ore body. In this study, however, the absence of magnetite + K-feldspar prevents the direct application of the experimental results.

A number of localities having the assemblage biotite–sulfide–magnetite are reported in the literature, but quantitative studies of biotite composition from these areas are rarely reported. Moh *et al.* (1964) and Harvey (1975) reported such an assemblage at Ducktown, Tennessee, which qualitatively indicates a higher content of Mg relative to Fe in biotites closer to the ore body. At Ore Knob, North Carolina, Fullager *et al.* (1977) have related an increase in the index of refraction of biotite to distance from the ore body.

Caution should, of course, be exercised before applying the experimental results to natural systems. Unless an oxygen fugacity-indicating mineral assemblage is present, estimation of location on a $\log fO_2$–$\log fS_2$ plot is uncertain. The importance of noting carefully the oxide and sulfide phases is obvious. The presence of graphite, for example, indicating a vapor containing species such as CO_2, CH_4, *etc.*, leads to further complications. These more complex fluids would likely have decreased fH_2 relative to the C-free system, and therefore decreased fH_2O, limiting the biotite stability field relative to that found in the H–O–S system.

Biotite compositions in this experimental study probably do not differ very much from those along the annite–phlogopite join, and if such slight deviations exist, the effect on the physical properties of the biotites is negligible. In the more complex chemical systems of natural rocks, the solid solution of additional elements in biotite, magnetite, or sulfide could complicate the application of our experimental results. Thus, many natural biotites contain significant amounts of $Al^{VI}Al^{IV}$ substituting for Fe^{VI} and Si^{IV}. Rutherford (1973) suggested that such a substitution would result in an increase of biotite stability relative to T and fO_2 in the same manner as the substitution of Mg^{VI} for Fe^{VI}(Wones and Eugster, 1965). Nevertheless, we hope that at least a simple approximation

allowing comparison of the natural samples with our experimental results can be used once the biotite compositions have been determined. The effect of substitutions of Cu, Ni, Co, *etc.* on sulfide–biotite relations has been neglected.

The experimental data are inconclusive for the effects of temperature and total pressure on the relationship between biotite and pyrrhotite. Popp *et al.* (1977) indicate, however, that for orthoamphibole-pyrrhotite there is no appreciable change in the silicate–sulfide compositions relative to one another in the range 650°–700°C at 2000 bars. No bracketing experiments at pressures other than 2000 bars have been attempted in our study. Wones and Eugster (1965) demonstrated that the pressure has a negligible effect on the composition of biotite–magnetite-K-feldspar equilibrium, and the effect on pyrrhotite vapor is likewise small. We believe, therefore, that differences in P_T will have little effect on the experimentally-determined equilibria.

In summary, a careful physical and chemical examination of all the phases present in an assemblage must be made. Additional experimental studies of sulfide–silicate reactions are obviously needed to further clarify such complex questions as the effect of various cationic substitutions in both silicates and sulfides, the effect of a more complex vapor composition, and the effect of differing temperatures on the reactions.

References

Annersten, H. (1969) Magnetites from a sulphide bearing iron ore formation in Sweden. *Mineral. Deposita, 4*, 234–240.

Bachinski, D. J. (1976) Metamorphism of cupriferous iron sulfide deposits, Notre Dame Bay, Newfoundland. *Econ. Geol., 71*, 443–452.

Banks, N. G. (1973) Biotite as a source of some sulfur in porphyry copper deposits. *Econ. Geol., 68*, 697–708.

Beane, R. E. (1974) Biotite stability in the porphyry copper environment. *Econ. Geol., 69*, 241–256.

Borg, I. Y. and D. K. Smith (1969) *Calculated X-ray Powder Patterns for Silicate Minerals.* Geol. Soc. Am. Mem. 122.

Burnham, C. W., J. R. Hollaway and N. F. Davis (1969) Thermodynamic properties of water to 1000°C and 10,000 bars. *Geol. Soc. Am. Spec. Pap. 132.*

Clark, T. and A. J. Naldrett (1972) The distribution of Fe and Ni between synthetic olivine and sulfide at 900°C. *Econ. Geol., 67*, 939–952.

Eugster, H. P. and G. Skippen (1967) Igneous and metamorphic

reactions involving gas equilibria. In P. H. Abelson, Ed., *Researches in Geochemistry, Vol. 2*, p. 402–520. Wiley, New York.

—— and D. R. Wones (1962) Stability relations of the ferruginous biotite, annite. *J. Petrol., 3*, 82–125.

Fullagar, P. D., H. S. Brown and A. F. Hagner (1967) Geochemistry of wall rock alteration and the role of sulfurization in the formation of the Ore Knob sulfide deposit. *Econ. Geol., 62*, 798–825.

Guidotti, C. V. (1970) The mineralogy and petrology of the transition from the lower to upper sillimanite zone in the Oquossoc area, Maine. *J. Petrol., 11*, 277–336.

Hammarbäck, S. and B. Lindqvist (1972) The hydrothermal stability of annite in the presence of sulfur. *Geol. Fören. Förh., 94*, 549–564.

Harvey, C. S. C. (1975) *Petrography, Structure and Trace Element Content of Wall Rock Biotites from the Boyd and Calloway Ore Bodies, Ducktown, Tennessee.* M. S. Thesis, North Carolina State University, Raleigh, N. C.

Hewitt, D. A. (1978) A redetermination of the fayalite–magnetite–quartz equilibrium between 650–850°C. *Am. J. Sci., 278*, 715–724.

—— and D. R. Wones (1975) Physical properties of some synthetic Fe–Mg–Al trioctahedral biotites. *Am. Mineral., 60*, 854–862.

Hougen, O. A., K. M. Watson and R. A. Ragatz (1964) *Chemical Process Principle Charts,* third edition. Wiley, New York.

Huebner, J. S. (1971) Buffering techniques for hydrostatic systems at elevated pressures. In G. Ulmer, Ed., *Research Techniques for High Pressure and High Temperature*, p. 173–177. Springer-Verlag, New York.

JANAF Thermochemical Tables (1971) *Natl. Stand. Ref. Data Service Nat. Bur. Stand. 37.*

Kullerud, G. and H. S. Yoder (1963) Sulfide–silicate relations. *Carnegie Inst. Wash. Year Book, 62*, 215–218.

—— and —— (1964) Sulfide–silicate relations. *Carnegie Inst. Wash. Year Book, 63*, 218–222.

Moh, G. H., G. Kullerud, O. Kingman and R. Diffenbach (1964) Studies of Ducktown, Tennessee ores and country rocks. *Carnegie Inst. Wash. Year Book, 63*, 211–213.

Naldrett, A. J. and G. M. Brown (1968) Reaction between pyrrhotite and enstatite–ferrosilite solid solutions. *Carnegie Inst. Wash. Year Book, 66*, 427–429.

Popp, R. K., M. C. Gilbert and J. R. Craig (1977) Stability of Fe–Mg amphiboles with respect to sulfur fugacity. *Am. Mineral., 62*, 13–20.

Putnam, G. W. (1972) Base metal distribution in granitic rocks: data from the Rocky Hill and Lights Creek Stocks, California. *Econ. Geol., 67*, 511–527.

—— (1973) Biotite–sulfide equilibria in granitic rocks; a revision. *Econ. Geol., 68*, 884–891.

Rajamani, V. (1976) Distribution of iron, cobalt, and nickel between synthetic sulfide and orthopyroxene at 900°C. *Econ. Geol., 71*, 795–802.

Robinson, P. and R. J. Tracy (1977) Sulfide–silicate–oxide equilibria in sillimanite–K-feldspar grade pelitic schists, central Massachusetts (abstr.). *EOS, 58*, 524.

Rutherford, M. J. (1973) The phase relations of aluminous iron biotites in the system $KAlSi_3O_8$–$KAlSiO_4$–Al_2O_3–Fe–O–H. *J. Petrol., 14*, 159–180.

Ryzhenko, B. N. and V. P. Volkov (1971) Fugacity coefficients of some gases in a broad range of temperatures and pressures. *Geokhimiya, 7*, 760–773 [transl. *Geochem. Int., 8*, 468–481 (1971)].

Schairer, J. F. and N. L. Bowen (1955) The system K_2O–Al_2O_3–SiO_2. *Am. J. Sci., 253*, 681–746.

Shaw, H. R. and D. R. Wones (1964) Fugacity coefficients for hydrogen gas between 0° and 1000°C, for pressures to 3000 atm. *Am. J. Sci., 262*, 918–929.

Staten, W. T. (1976) *A Chemical Study of the Silicate Minerals of the Great Gossan Lead and Surrounding Rocks in Southwestern Virginia.* M. S. Thesis, Virginia Polytechnic Institute and State University, Blacksburg, Virginia.

Toulmin, P. and P. B. Barton (1964) A thermodynamic study of pyrite and pyrrhotite. *Geochim. Cosmochim. Acta, 28*, 641–671.

Tso, J. L. (1977) *Sulfidation of Synthetic Biotites.* M. S. Thesis, Virginia Polytechnic Institute and State University, Blacksburg, Virginia.

Wones, D. R. (1963) Physical properties of synthetic biotites on the join phlogopite–annite. *Am. Mineral., 48*, 1300–1321.

—— (1972) Stability of biotite: a reply. *Am. Mineral., 57*, 316–317.

—— and H. P. Eugster (1965) Stability of biotite: experiment, theory and application. *Am. Mineral., 50*, 1228–1272.

Yund, R. A. and H. T. Hall (1969) Hexagonal and monoclinic pyrrhotites. *Econ. Geol., 64*, 420–423.